S-(carboxymethyl)cysteine, 638-23-3.

REFERENCES

Allison, J., & Kaplan, N. O. (1964) *J. Biol. Chem. 239*, 2140–2152.

Ellenrieder, G. V., Kirschmer, K., & Schuster, I. (1972) *Eur. J. Biochem. 26*, 220–235.

King, L., & Weber, G. (1986a) *Biochemistry 25*, 3632–3637.

King, L., & Weber, G. (1986b) *Biochemistry 25*, 3637–3640.

Kirschner, K., & Voigt, B. (1968) *Hoppe Seyler's Z. Physiol. Chem. 349*, 632–644.

Liddington, R., Derewenda, Z., Dodson, G., & Harris, D. (1988) *Nature 331*, 725–728.

Monod, J., Wyman, J., & Changeux, J.-P. (1965) *J. Mol. Biol. 12*, 88–118.

Mueller, K., Luedemann, H.-D., & Jaenicke, R. (1981) *Biochemistry 20*, 5411–5416.

Paladini, A. A., & Weber, G. (1981a) *Rev. Sci. Instrum. 52*, 419–427.

Paladini, A. A., & Weber, G. (1981b) *Biochemistry 20*, 2587–2593.

Perutz, M. F. (1970) *Nature 228*, 726–739.

Reinhart, G., & Hartleip, S. (1986) *Biochemistry 26*, 7308–7313.

Royer, C. A. (1985) Ph.D. Thesis, University of Illinois.

Ruan, K., & Weber, G. (1988) *Biochemistry 27*, 3295–3301.

Silva, J. L., Miles, E. W., & Weber, G. (1986) *Biochemistry 25*, 5781–5786.

Smith, F., Gingrich, D., Hoffman, B. M., & Ackers, G. K. (1988) *Proc. Natl. Acad. Sci. U.S.A. 84*, 7089–7093.

Stacel, G. M., & Deal, W. C. (1968) *Biochem. Biophys. Res. Commun. 31*, 398–403.

Valeur, B., & Weber, G. (1977) *Photochem. Photobiol. 25*, 441–444.

Weber, G. (1986) *Biochemistry 25*, 3626–3631.

Weber, G. (1987) *NATO ASI Ser., Ser. C No. 197*, 401–420.

Xu, G.-J., & Weber, G. (1982) *Proc. Natl. Acad. Sci. U.S.A. 79*, 5268–5271.

EPR Characterization of the Iron–Sulfur-Containing NADH–Ubiquinone Oxidoreductase of the *Escherichia coli* Aerobic Respiratory Chain†

Steven W. Meinhardt,‡ Kazunobu Matsushita,§,‖ H. Ronald Kaback,§ and Tomoko Ohnishi*,‡

Department of Biochemistry and Biophysics, University of Pennsylvania, Philadelphia, Pennsylvania 19104, and Roche Institute of Molecular Biology, Roche Research Center, Nutley, New Jersey 07110

Received June 1, 1988; Revised Manuscript Received October 20, 1988

ABSTRACT: The energy coupled NADH–ubiquinone (Q) oxidoreductase segment of the respiratory chain of *Escherichia coli* GR19N has been studied by EPR spectroscopy. Previously Matsushita et al. [(1987) *Biochemistry 26*, 7732–7737] have demonstrated the presence of two distinct NADH–Q oxidoreductases in *E. coli* membrane particles and designated them NADH dh I and NADH dh II. Although both enzymes oxidize NADH, only NADH dh I is coupled to the formation of the H^+ electrochemical gradient. In addition to NADH, NADH dh I oxidizes nicotinamide hypoxanthine dinucleotide (deamino-NADH), while NADH dh II does not. In membrane particles we have detected EPR signals arising from four low-potential iron–sulfur clusters, one binuclear, one tetranuclear, and two fast spin relaxing $g_\perp = 1.94$ type clusters (whose cluster structure has not yet been assigned). The binuclear cluster, temporarily designated $[N\text{-}1]_E$, shows an EPR spectrum with $g_{x,y,z} = 1.92, 1.935, 2.03$ and the $E_{m7.4}$ value of −220 mV ($n = 1$). The tetranuclear cluster, $[N\text{-}2]_E$, elicits a spectrum with $g_{x,y,z} = 1.90, 1.91, 2.05$ and an $E_{m7.4}$ of −240 mV ($n = 1$). These two clusters have been shown to be part of the NADH dh I complex by stability and inhibitor studies. When stored at 4 °C, both clusters are extremely labile as is the deamino-NADH–Q oxidoreductase activity. Addition of deamino-NADH in the presence of piericidin A results in nearly full reduction of $[N\text{-}2]_E$ within 17 s. In membrane particles pretreated with piericidin A, the cluster $[N\text{-}1]_E$ is only partly reducible by deamino-NADH and shows an altered line shape. The two remaining fast relaxing iron–sulfur clusters, $[N\text{-}3a]_E$ ($g_\perp = 1.94$, $g_\parallel = 2.02$) and $[N\text{-}3b]_E$ ($g_\perp = 1.94$, $g_\parallel = 2.03$), have an $E_{m7.4}$ of −260 mV ($n = 2$). These clusters may also be part of the NADH–Q oxidoreductase since in the mutant IY91, which possesses a very low level of deamino-NADH–Q oxidoreductase activity, they are modified in both their redox and spectral properties as is the $g_x = 1.90$ signal of the cluster $[N\text{-}2]_E$.

In *Escherichia coli*, the nature of the membrane-bound NADH–ubiquinone (Q) oxidoreductase (previously referred to as NADH dehydrogenase) and its role in the formation of a proton electrochemical gradient ($\Delta\tilde{\mu}_{H^+}$) have remained unresolved for many years. Early studies into the nature of the NADH dehydrogenase have indicated the presence of multiple enzymes with NADH dehydrogenase activity. In deoxycholate extracts from *E. coli* membrane particles, Bragg and Hou (1967) suggested the presence of two different NADH dehydrogenase enzymes on the basis of their substrate and inhibitor specificity. Gutman et al. (1968) studied a NADH dehydrogenase that was released from membrane particles by lyophilization and rehydration. They demonstrated the presence of non-heme iron and acid-labile sulfur as well as flavin in this preparation. Hendler and Burgess (1974)

† Supported by NIH Grant GM 30736 to T.O. and National Research Service Award GM 11165 to S.W.M.

* Author to whom correspondence should be addressed.

‡ University of Pennsylvania.

§ Roche Institute of Molecular Biology.

‖ Present address: Department of Agricultural Chemistry, Faculty of Agriculture, Yamaguchi University, Yamaguchi 753, Japan.

0006-2960/89/0428-2153$01.50/0

characterized the deoxycholate-extracted NADH dehydrogenase and found three separate peaks of NADH dehydrogenase activity. They showed the presence of iron in one peak fraction but found very low iron concentrations in other peaks. Immunoelectrophoresis studies by Owen et al. (1979, 1980) also demonstrated the presence of two to three distinct enzymes with NADH dehydrogenase activity. In their preparations, one of the antigenically active proteins, no. 15, was shown to contain iron. Concurrently, Ingledew et al. (1980) demonstrated the presence of two low-potential iron–sulfur clusters, E_m = −220 and −250 mV, in membrane particles.

A controversy over the nature of the NADH dehydrogenase arose when Young et al. (1978) reported the isolation of the NADH dehydrogenase gene and its amplification in a strain of *E. coli* lacking any NADH dehydrogenase activity. The NADH dehydrogenase isolated from the amplified strain was found to be composed of a single polypeptide with a molecular weight of 47000 (Jaworowski et al., 1981a). It was shown to contain one tightly bound FAD and approximately one ubiquinone but no iron (Jaworowski et al., 1981b).

Whether any of the NADH dehydrogenase(s) found in the membrane was coupled to the generation of a $\Delta\tilde{\mu}_{H^+}$ (ATP production) or not has also been controversial. Studies of the growth yields of *E. coli* cells under sulfur (Poole & Haddock, 1975) or iron (Rainnie & Bragg, 1973) limitation indicated the presence of site I energy coupling in normal cells. Brookman et al. (1979) also showed that NADH–menadione reductase activity was coupled to proton translocation. However, they concluded that the proton translocation that they initially observed was due to a membrane-bound adenosine triphosphatase and that NADH–menadione oxidoreductase was not involved in proton translocation.

These controversies have remained unresolved until recent work by Matsushita et al. (1986, 1987), demonstrating the presence of two distinct species of the NADH dehydrogenase (NADH dh I and NADH dh II) in *E. coli* cytoplasmic membranes. The two enzymes were distinguished by their differences in substrate specificity, inhibitor sensitivity, and stability. NADH dh I, which is extremely unstable, oxidizes both NADH and nicotinamide hypoxanthine dinucleotide (deamino-NADH) and forms a $\Delta\tilde{\mu}_{H^+}$ coupled with its electron transfer to Q_1. This enzyme is more sensitive to inhibition by piericidin A or 3-undecyl-2-hydroxy-1,4-naphthoquinone (UHNQ) and has a lower K_m for NADH in comparison to the NADH dh II. The latter enzyme, which is more stable and oxidizes only NADH, is not coupled to the formation of a proton electrochemical gradient. It is presumably the enzyme that was previously isolated by Jaworowski et al. (1981a,b).

In this paper we have extended the EPR characterization of the NADH dh I segment of the respiratory chain in membrane particles of *E. coli* GR19N. We show here that NADH dh I contains at least two distinct low-potential iron–sulfur clusters. The physicochemical properties of the additional two low-potential iron–sulfur clusters are also presented. Preliminary results have been reported previously (Ohnishi et al., 1986, 1987).

Materials and Methods

NADH and deamino-NADH were purchased from Sigma. 3-Undecyl-2-hydroxy-1,4-naphthoquinone was obtained from Aldrich. All other chemicals were of reagent grade and were obtained from commercial sources.

E. coli strains GR19N (cyd$^-$) (Green & Gennis, 1983) and IY91 were grown as described previously (Matsushita & Kaback, 1986) and stored as a frozen cell paste at −80 °C until use. Membrane particles were prepared by resuspending 25 g of the cell paste in 125 mL of 50 mM potassium phosphate, 5 mM magnesium sulfate, and 0.5 mM EDTA (pH 7.4) (buffer A) and centrifuged at 10000*g* for 20 min. The pellet was resuspended in the following buffer, 50 mM potassium phosphate, 5 mM magnesium sulfate, 0.5 mM EDTA, 2 mM dithiothreitol, and 10% glycerol (pH 7.4) (buffer B). The cells were broken by two passes through an Aminco french press at 20000 psi and then centrifuged at 15000*g* for 10 min. The supernatant was retrieved, and an equal volume of buffer B was added. The supernatant was centrifuged at 50000*g* for 90 min. The pellet was resuspended in 110 mL of 50 mM potassium phosphate, 5 mM magnesium sulfate, 0.5 mM EDTA, 2 mM dithiothreitol, and 5% glycerol (pH 7.4) (buffer C) and centrifuged a second time at 50000*g* for 90 min. The final pellet was resuspended in a minimal volume of buffer C and stored at −80 °C until use. Redox titrations were performed as described by Dutton (1978). Spectra were recorded on a Varian E-109 EPR spectrometer connected to a dedicated IBM-PC for data acquisition and manipulation.

The *g* values reported here were obtained directly from the recorded spectra except for $[N\text{-}2]_E$.[1] The *g* values for this iron–sulfur cluster were obtained from simulation of the spectrum. EPR spectra of the separate clusters used for simulation were obtained under non-power-saturating conditions. Simulations assumed Gaussian line shapes and no hyperfine interactions as described by Blum and Ohnishi (1980). The magnetic field sweep was divided into 500 points and integration around the angles θ and ϕ was performed in 200 loops. Spectral simulations were calculated by using the University of Pennsylvania, School of Medicine, VAX 8600 computer (Digital Electronics Corp., Maynard, MA).

Results

Resolution of the EPR Spectra of Iron–Sulfur Clusters in Cytoplasmic Membrane Particles. In Figure 1 we show the spectra obtained from freshly prepared *E. coli* GR19N membrane particles reduced either with succinate or with both succinate and NADH, under two sets of EPR conditions (traces A and B). At the sample temperature of 25 K and a microwave power of 1 mW, signals arising from binuclear clusters predominate. After reduction with succinate, Figure 1A (dashed line), a rhombic spectrum was observed with $g_{x,y,z}$ = 1.91, 1.935, 2.03, which is very similar to the cluster [S-1] spectrum seen in succinate-reduced bovine heart submitochondrial particles. These signals most likely arise from the binuclear iron–sulfur cluster, $[S\text{-}1]_E$, present in the succinate dehydrogenase. When NADH is added to the particles together with succinate [Figure 1A (solid line)], a spectrum with less rhombicity emerged with *g* values of $g_{x,y,z}$ = 1.92, 1.935, 2.03. This spectrum resembles that of the cluster [N-1b] in the bovine heart NADH–Q oxidoreductase (Hearshen et al., 1981), and we have designated it the cluster $[N\text{-}1]_E$. The isotropic g = 2.005 signals seen in all the spectra of Figure 1 have a peak to peak width of 1.2–1.4 × 10^{-3} T. These signals are most likely the overlapped signals arising from either the semiquinone or the flavosemiquinone radicals in the respiratory chain.

To examine signals from tetranuclear clusters that exhibit, in general, much faster spin relaxation than binuclear clusters, the EPR spectra were recorded at 11 K, with the microwave

[1] For the convenience of the readers we have given the iron–sulfur clusters simplified names with the subscript E to designate that they are found in *Escherichia coli*.

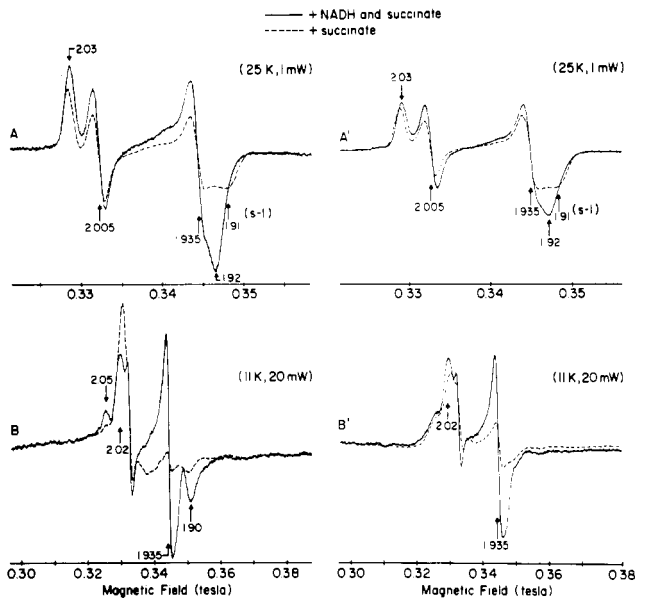

FIGURE 1: EPR Spectra of *E. coli* GR19N membrane particles, reduced with succinate alone or with succinate and NADH, recorded under two different EPR conditions. *E. coli* GR19N membrane particles were suspended in buffer A described under Materials and Methods. Succinate (10 mM final concentration) or NADH (5 mM final concentration) together with succinate (10 mM) was added as depicted in the figure. The EPR conditions were as shown in the figure with a modulation amplitude of 1.25×10^{-3} T, a time constant of 0.128 s, and a scan rate of either 1.0×10^{-2} T/min (A and A′) or 2.5×10^{-2} T/min (B and B′).

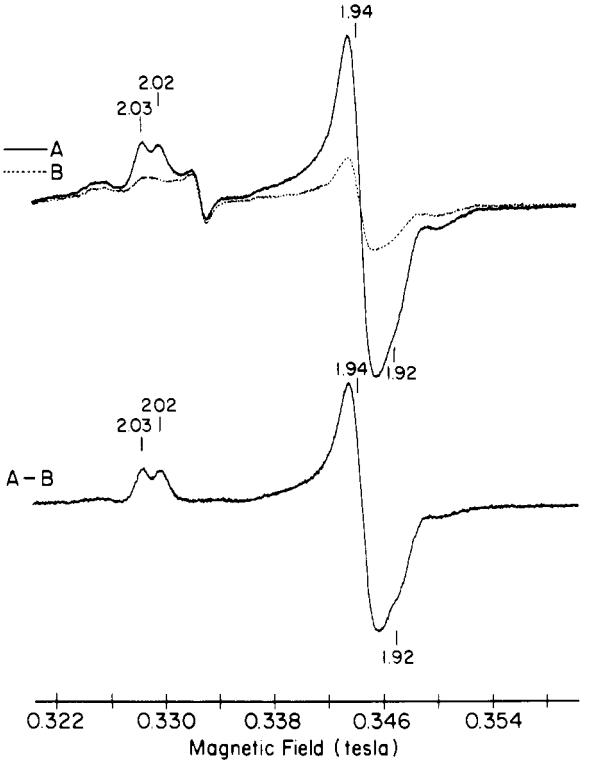

FIGURE 2: Potentiometrically resolved spectra of the clusters $[N\text{-}3a]_E$ and $[N\text{-}3b]_E$ of *E. coli*. *E. coli* GR19N membrane particles were suspended in buffer C to a concentration of 54 mg of protein/mL and the following redox mediators were added: 40 μM each of methyl viologen, benzylviologen, phenosafranine O, indigo disulfonate, and indigo trisulfonate, and 10 μM pyocyanine. (A) The particles were redox poised at the E_h value of −264 mV. (B) The particles were poised at −231 mV. EPR conditions: microwave power, 10 mW; modulation amplitude, 6.3×10^{-4} T; scan rate, 2.0×10^{-2} T/min; time constant, 0.064 s; sample temperature, 11 K. The spectra are an average of four scans.

power setting of 20 mW. In this case, membrane particles reduced with succinate [Figure 1B (dotted line)] showed a partially saturated $[S\text{-}1]_E$ signal and the $g_z = 2.02$ signal arising from the cluster $[S\text{-}3]_E$ of the succinate dehydrogenase that is EPR detectable in the oxidized state. The addition of NADH and succinate[2] to the particle suspension [Figure 1B (solid line)] resulted in the appearance of signals at $g = 2.05$, 2.02, 1.935, and 1.90. These signals represent at least two separate iron–sulfur species, since the $g = 1.90$ and 2.05 signals exhibit the power saturation parameter, $P_{1/2}$, of approximately 20 mW at 11 K, which is considerably different from the $P_{1/2}$ of the $g = 1.935$ and 2.02 signals, i.e., 0.3 mW at the same sample temperature. We have named these two low-temperature-detectable iron–sulfur species clusters $[N\text{-}2]_E$ and $[N\text{-}3]_E$, respectively. In Figure 2 we will further resolve the $[N\text{-}3]_E$ ($g = 1.935$, 2.02) signals into two distinct EPR species.

Previously it has been shown that the piericidin A sensitive, energy-transducing NADH dh I is extremely unstable (Matsushita et al., 1987). When *E. coli* membrane particles were stored overnight at 4 °C, more than 50% of the deamino-NADH oxidase activity was lost with no significant change in the NADH and succinate oxidase activities. As an initial survey for the presence of iron–sulfur clusters in the NADH dh I complex, we have examined EPR spectra of membrane particles that have been stored overnight at 4 °C [Figure 1 (traces A′ and B′)]. When these particles were reduced with succinate [Figure 1A′ (dashed line)], the spectrum from the cluster $[S\text{-}1]_E$ was seen at approximately the same concentration as in the fresh membrane sample. The addition of NADH together with succinate [Figure 1A′ (solid line)] resulted in the reduction of the cluster $[N\text{-}1]_E$, but at a much lower spin concentration relative to the cluster $[S\text{-}1]_E$ than seen in the freshly prepared membrane particles (Figure 1A). A 11 K and 20 mW, the succinate-reduced aged sample showed an altered line shape with a prominent shoulder at $g = 2.04$ and a slightly altered line shape of $g_y g_x$ negative trough region when compared with the counterparts in the freshly prepared membrane particles [Figure 1B′ (dotted line)]. The most evident change in the low-temperature spectra of the aged particles is the almost complete absence of the cluster $[N\text{-}2]_E$ signals ($g_x = 1.90$ and $g_z = 2.05$) that are obtained for NADH-reduced samples. An alternative interpretation for the appearance of the $g = 2.04$ signal in spectra B′ is that both line shape and the E_m of the cluster $[N\text{-}2]_E$ were altered and that its spectrum was already included in the succinate-reduced spectrum [Figure 1B′ (dotted line)]. The addition of NADH to the membrane particles also resulted in the appearance of signals with roughly axial symmetry ($g_\perp = 1.935$ and $g_\parallel = 2.02$). The amplitude of the $g_\perp = 1.935$ signal was again diminished relative to that of the partially saturated $[S\text{-}1]_E$ signals, probably due to a slight spectral broadening [Figure 1B′ (dashed line)].

A more detailed spectral resolution of the cluster $[N\text{-}3]_E$ species was conducted by using potentiometrically poised samples recorded at 11 K with an expanded field scale (see Figure 2). This figure presents the spectra of samples poised at −264 (A) and −231 mV (B), pH 7.4, obtained during a reductive titration. When the modulation amplitude was reduced to 6.3×10^{-4} T to enhance the spectral resolution, the g_z peak was clearly resolved into two peaks, one at $g_z = 2.02$,

[2] In some *E. coli* GR19N membrane particle preparations, NADH was found to be a much weaker reductant of the cluster $[S\text{-}3]_E$ than succinate. Thus, succinate was added together with NADH to avoid interference of the cluster $[S\text{-}3]_E$ spectrum with the g_z signals of the low E_m iron–sulfur clusters [for example, see Figure 7B (dotted line)].

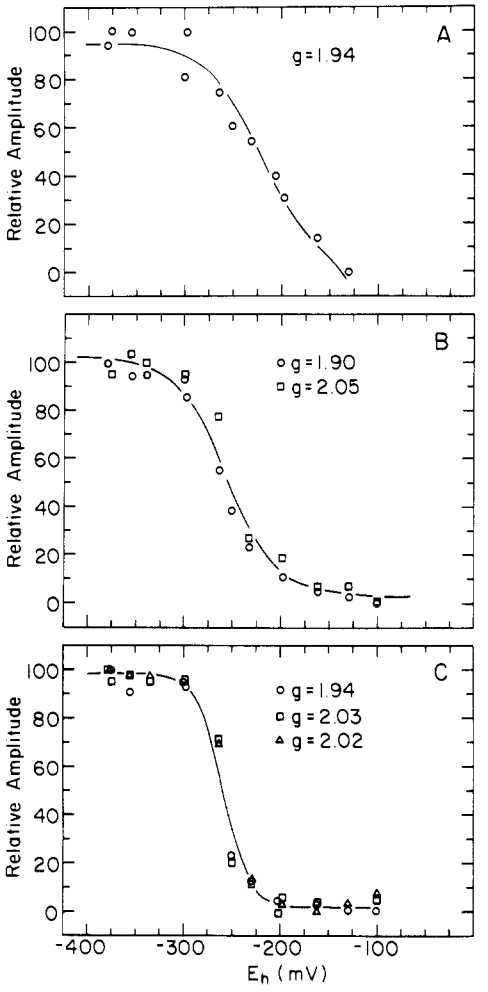

FIGURE 3: Redox titrations of the low-potential iron–sulfur clusters of *E. coli*. *E. coli* membrane particles were suspended in buffer C to a concentration of 54 mg of protein/mL with the same redox mediators as in Figure 2. During a reductive titration, EPR samples were made at the potentials indicated. The g = 1.94 signal was measured from the peak to the trough. All other signals were measured from the base line to the peak. (A) The EPR conditions were as follows: microwave power, 1 mW; scan rate, 0.01 T/min; modulation amplitude, 6.3 × 10^{-4} T; time constant, 0.25 s; temperature, 26 K. Through the data is drawn a two-component redox titration curve with midpoints of −42 mV, n = 1, and −221 mV, n = 1. (B) The EPR conditions were the same as in (A) except the microwave power (10 mW), the temperature (11 K), and the time constant (0.128 s). Through the data is drawn a single-component redox titration curve with a midpoint of −257 mV, n = 1. (C) The EPR conditions were as in (B). Through the data is drawn a single-component redox titration curve with a midpoint of −260 mV, n = 2.

the other at g_z = 2.03. We distinguish these two resolved iron–sulfur species as the clusters $[N\text{-}3a]_E$ and $[N\text{-}3b]_E$, respectively. Both signals showed similar power saturation characteristics and, as shown below, titrated with the same redox properties. The presence of two iron–sulfur clusters is also indicated by the spectral line shape in the g = 1.94–1.92 region, which cannot be simulated as a single component.

From the spectra presented in Figures 1 and 2 we have demonstrated the presence of at least four distinct iron–sulfur clusters, which are reducible by NADH but not by succinate. Of these four, two clusters, namely, the tetranuclear cluster $[N\text{-}2]_E$ and the binuclear cluster $[N\text{-}1]_E$, showed a marked modification when the deamino-NADH–Q reductase activity was lost.

Redox Properties of the Iron–Sulfur Clusters. Figure 3A shows a redox titration of the g = 1.94 signal measured under the conditions in which signals from binuclear clusters predominate. This signal titrated as a one-electron oxidation reduction curve with a midpoint potential of −220 mV (pH 7.4). Not plotted is the change due to the iron–sulfur cluster $[S\text{-}1]_E$, which has an $E_{m7.4}$ of −40 mV in this preparation. The −220-mV species represented only 20% of the total signal change in this titration. Figure 3B shows titrations of the g = 2.05 and 1.90 signals recorded at 11 K and 20 mW. The g = 2.05 signal titrated as an n = 1 oxidation reduction couple with an $E_{m7.4}$ of −240 mV. The g = 1.90 signal also titrated as an n = 1 component with a slightly lower midpoint potential, $E_{m7.4}$ = −260 mV. Since the amplitude that we have measured for this signal was affected by the much larger signal with $g_\perp$ = 1.94, which titrated with a midpoint of −260 mV, we do not consider the E_m values monitored at g = 1.90 and 2.05 to be significantly different. Figure 3C shows the titration of the signals at g = 2.03, 2.02, and 1.94. All three signals titrated with an $E_{m7.4}$ of −260 mV and n = 2 oxidation reduction curve. The difference in n value obtained from the titration of the 2.03 signal at 11 K (Figure 3C) and at 25 K (Figure 3A) indicates that the $[N\text{-}1]_E$ and $[N\text{-}3b]_E$ are two distinct iron–sulfur species and that the $[N\text{-}3b]_E$ signal detected at 11 K does not arise from the partially power saturated binuclear $[N\text{-}1]_E$ cluster.

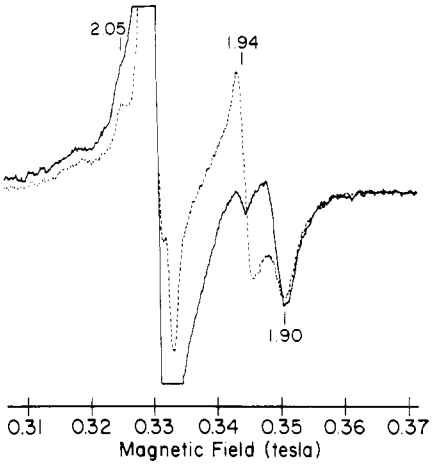

FIGURE 4: Effect of piericidin A on the reduction of the low-temperature-detectable iron–sulfur clusters. *E. coli* membrane particles were suspended in buffer C to a concentration of 75 mg of protein/mL. Samples were incubated for 3 min after the addition of 5 mM deamino-NADH and then frozen. (Solid line) Membrane particles were preincubated with piericidin A (50 nmol/mg of protein) for 2.5 min in ice prior to the addition of 5 mM deamino-NADH. (Dashed line) No inhibitor was added. Both spectra were recorded under the following EPR conditions: microwave power, 20 mW; scan rate, 2.5 × 10^{-2} T/min; modulation amplitude, 1 × 10^{-3} T; time constant, 0.128 s; microwave frequency, 9.323 GHz; sample temperature, 11 K. Both traces are an average of four scans.

Assignment of the Iron–Sulfur Clusters to NADH dh I. An iron–sulfur cluster can be shown to be part of the NADH dh I complex more definitively if it is reduced by deamino-NADH in the presence of an inhibitor that prevents electron transfer to the quinone pool. We have examined membrane particles treated with piericidin A, a quinone analogue that is a potent inhibitor of this complex, prior to the addition of deamino-NADH. We have also performed similar experiments using 3-undecyl-2-hydroxy-1,4-naphthoquinone (UHNQ), which is a general quinone site inhibitor and has multiple inhibition sites in the *E. coli* aerobic electron transport chain.

In Figure 4 are shown spectra, recorded at 11 K, obtained from membrane particles reduced with deamino-NADH either in the absence (dotted line) or in the presence (solid line) of piericidin A. When deamino-NADH is added to membrane particles without inhibitor pretreatment, both $[N\text{-}3]_E$ and

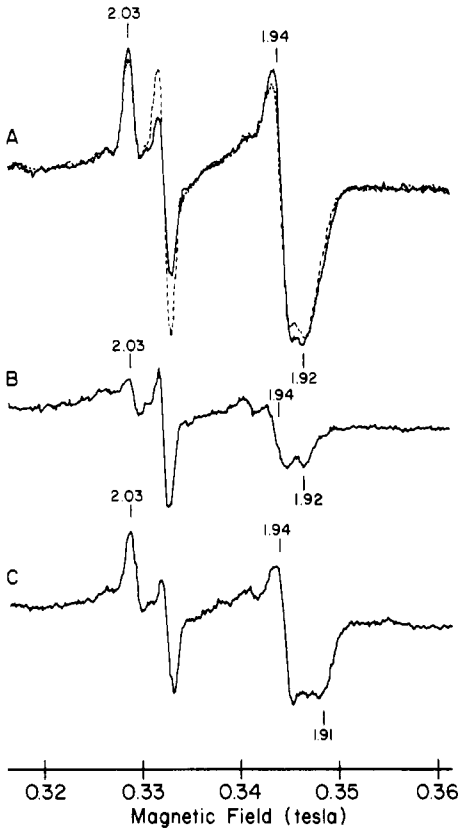

FIGURE 5: Spectral resolution of the low-potential binuclear iron–sulfur cluster $[N\text{-}1]_E$ utilizing piericidin A. *E. coli* membrane particles were suspended in the same manner as in Figure 4. (A) (Solid line) 10 mM L-lactate was added and the sample incubated for 10 min prior to freezing. (Dashed line) The sample was incubated for 2.5 min after the addition of 5 mM deamino-NADH. (B) Piericidin A (50 nmol/mg of protein) was added 2.5 min prior to the addition of 5 mM deamino-NADH. The sample was then incubated for 2.5 min before freezing. (C) Piericidin A was added as in (B), and 10 mM L-lactate was added. The sample was incubated for 2.5 min and then frozen. In all spectra, the EPR conditions were as follows: microwave power, 1 mW; modulation amplitude, 1.25×10^{-3} T; scan rate, 5×10^{-2} T/min; time constant, 0.064 s; sample temperature, 26 K.

$[N\text{-}2]_E$ clusters were reduced. If membrane particles were preincubated with piericidin A prior to the addition of deamino-NADH (solid line), only a minor portion (<10%) of the cluster $[N\text{-}3]_E$, $g_\perp = 1.94$, was reduced, while full reduction of the cluster $[N\text{-}2]_E$, $g_x = 1.90$, occurred. This result strongly indicates that the cluster $[N\text{-}2]_E$ is a component of the NADH dh I. It also shows that this tetranuclear cluster $[N\text{-}2]_E$ has a nearly axial symmetry with $g_{x,y,z}$ values of 1.90, 1.91, 2.05. Since both low-temperature-detectable clusters, $[N\text{-}3a]_E$ and $[N\text{-}3b]_E$, are not reduced by deamino-NADH in the piericidin A pretreated membrane particles, these two iron–sulfur clusters may not be part of the NADH dh I complex.

Spectra in Figure 5 were obtained with the samples reduced with either L-lactate or deamino-NADH in the presence or absence of piericidin A, recorded at 26 K and 1 mW. The L-lactate dehydrogenase, which is known to be an inducible enzyme, contains FMN and no iron–sulfur clusters (Futai & Kimura, 1977). Thus, these cells, which were grown with DL-lactate as a carbon source, exhibited a very high L-lactate dehydrogenase activity (Matsushita et al., 1987). Since the redox midpoint potential of lactate is relatively low ($E_m = -180$ mV, lactate/pyruvate), it has allowed us to reduce all of the iron–sulfur clusters in the membrane. Figure 5A shows that, in the absence of piericidin A pretreatment, either L-lactate or deamino-NADH fully reduces the binuclear clusters $[N\text{-}1]_E$ and $[S\text{-}1]_E$ after a 10-min incubation at room temperature. If particles were preincubated with piericidin A prior to the addition of deamino-NADH (Figure 5B), a rhombic binuclear cluster ($g_{x,y,z}$ = 1.92, 1.94, 2.03) was partly reduced. If L-lactate is added after preincubation with piericidin A (Figure 5C), the cluster $[S\text{-}1]_E$ with $g_{x,y,z}$ 1.91, 1.94, 2.03 was reduced. The spectrum of this cluster is the same as that seen in succinate-reduced particles, namely, cluster $[S\text{-}1]_E$ [Figure 1A (dotted line)]. In our *E. coli* membrane preparations, the binuclear iron–sulfur clusters reacted slowly with NADH or deamino-NADH with a half-time in the range of 1–2 min even in the presence of piericidin A. Assuming that only those iron–sulfur clusters that are not part of NADH dh I are reduced by L-lactate in the presence of piericidin A, about the half of the signal amplitude seen in Figure 5A is due to the cluster $[N\text{-}1]_E$. Therefore, in Figure 5B the amplitude of the signal represents only half of the total low-potential binuclear cluster $[N\text{-}1]_E$.

Although the above experiment indicates that the binuclear cluster is part of the NADH dh I complex, the line shape of the cluster reduced by deamino-NADH in the presence of piericidin A is considerably different from that seen in Figure 1A,A′. To analyze this effect further, we examined the redox state of this binuclear type cluster in the UHNQ-inhibited membrane system after the addition of substrates. UHNQ is a less specific inhibitor of the NADH dh I complex than piericidin A and has multiple inhibition sites. UHNQ at 100 nmol/mg of protein inhibited the quinol oxidase complexes most strongly (QH_2–O_2, 96% inhibition) followed by the NADH dh I complex (deamino-NADH–Q_1, 71%) and L-lactate dehydrogenase (L-lactate–Q_1, 55%) in decreasing order of inhibition (Matsushita et al., 1987). When the deamino-NADH was added to the membrane particles, after the 5-min preincubation with UHNQ (100 nmol/mg of protein), we obtained a spectrum composed of the $[N\text{-}1]_E$ and $[S\text{-}1]_E$ (Figure 6A). The spectrum is composed of both species, because the strongest inhibition site of UHNQ is at the QH_2–cyt *o* step with a weaker inhibition of the primary dehydrogenases. Therefore, the quinone pool becomes reduced due to the leak through the NADH dh I, resulting in the concomitant reduction of the cluster $[S\text{-}1]_E$. When L-lactate was added after UHNQ pretreatment (Figure 6B), only the cluster $[S\text{-}1]_E$ signal was seen after 5 min. Previously in Figure 5 we demonstrated that L-lactate is capable of reducing all of the iron–sulfur clusters in the absence of piericidin A inhibition. Therefore, the binuclear $[N\text{-}1]_E$ cluster, reduced by deamino-NADH, minus the contribution of $[S\text{-}1]_E$ is most likely part of NADH dh I. When we subtracted an appropriate fraction of spectrum 6B from the deamino-NADH-reduced sample (spectrum 6A), we obtained the spectrum of the cluster $[N\text{-}1]_E$ (Figure 6C), which can be simulated as a single iron–sulfur cluster with $g_{x,y,z}$ = 1.922, 1.935, 2.024 and $L_{x,y,z} = 6.4 \times 10^{-4}$, 7.7×10^{-4}, 9.45×10^{-4} T (Ohnishi et al., 1987). This spectrum is more similar to that obtained in the absence of inhibitors than that obtained in the presence of piericidin A. These results suggest that the spectrum of the binuclear cluster $[N\text{-}1]_E$ can be modified by the binding of a strong inhibitor, such as piericidin A, to the complex in the membrane. In contrast to the binuclear-type cluster $[N\text{-}1]_E$ of NADH dh I, the line shape of the tetranuclear type cluster $[N\text{-}2]_E$ did not appear to be affected by the binding of piericidin A (Figure 4).

Characteristics of the Mutation in IY91. The *E. coli* strain IY91 had been used previously to show that the NADH dehydrogenase was not coupled to the formation of an electrochemical membrane potential. This strain contains amplified

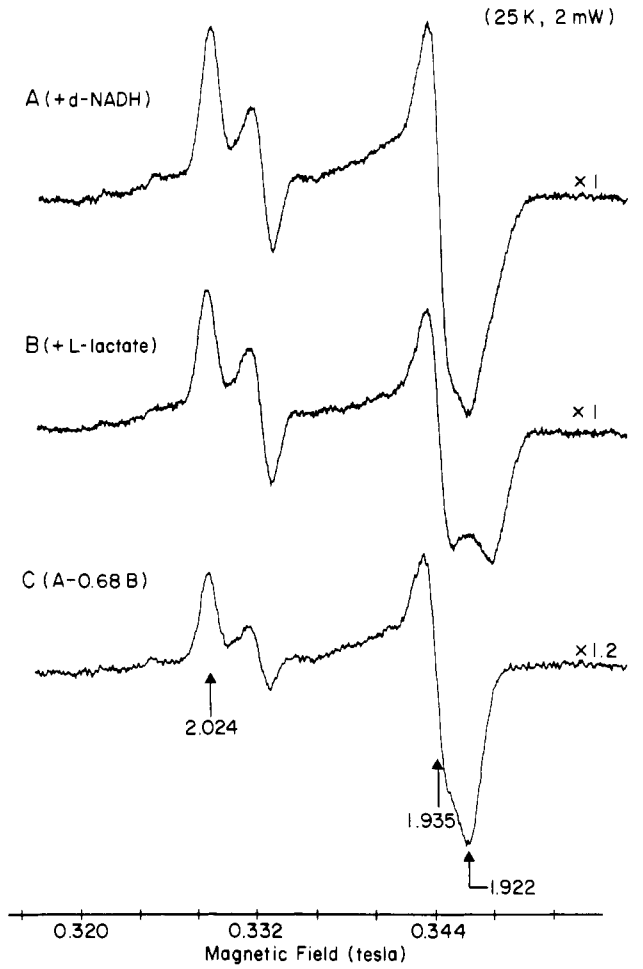

FIGURE 6: Spectral resolution of the low-potential binuclear iron–sulfur cluster with UHNQ. *E. coli* membrane particles (50 mg of protein/mL) were preincubated with UHNQ (100 nmol/mg of protein) for 5 min and then reduced with either 5 mM deamino-NADH (A) or 10 mM L-lactate (B). Spectrum C represents cluster $[N\text{-}1]_E$ in the NADH dh I that was obtained by subtracting an appropriate fraction of the cluster $[S\text{-}1]_E$ signal (0.68 × spectrum B) from spectrum A. This totally eliminated the $g = 1.91$ shoulder from spectrum C. EPR conditions: microwave power 2 mW; modulation amplitude 1.25×10^{-3} T; scan rate, 1×10^{-2} T/min; time constant, 0.0645 s; sample temperature, 25 K. All spectra are an average of four scans.

NADH dehydrogenase dh II (Jaworowski et al., 1981b) and was constructed from a mutant, IY12, lacking almost all NADH dehydrogenase activity (Young et al., 1978). It has subsequently been shown that IY91 strain is also almost completely devoid of deamino-NADH oxidase activity (Matsushita et al., 1987). We have prepared membrane particles from this mutant and have examined the EPR spectra of the iron–sulfur clusters. Figure 7 shows spectra obtained from IY91 upon reduction by succinate (dotted lines) or by NADH (solid lines). Relatively normal amounts of the binuclear clusters $[S\text{-}1]_E$ and $[N\text{-}1]_E$ are present, in comparison to the spectra in Figure 1, although both species showed somewhat altered line shapes in the g_x region. The difference in the g_x position of the succinate-reduced sample from that seen in Figure 1 could be due to a shift in the midpoint potential of the cluster $[N\text{-}1]_E$, which would allow the partial reduction of this cluster by succinate. Stronger line-shape alterations were discerned in the EPR spectra of the clusters $[N\text{-}2]_E$ and $[N\text{-}3]_E$, detected at 11 K. The $g_x = 1.90$ signal of the cluster $[N\text{-}2]_E$ has been shifted to a higher magnetic field, namely, to $g_x = 1.87$. In addition, this cluster has become fully reducible by either succinate or NADH, suggesting a large positive shift in its redox midpoint potential. The $g =$

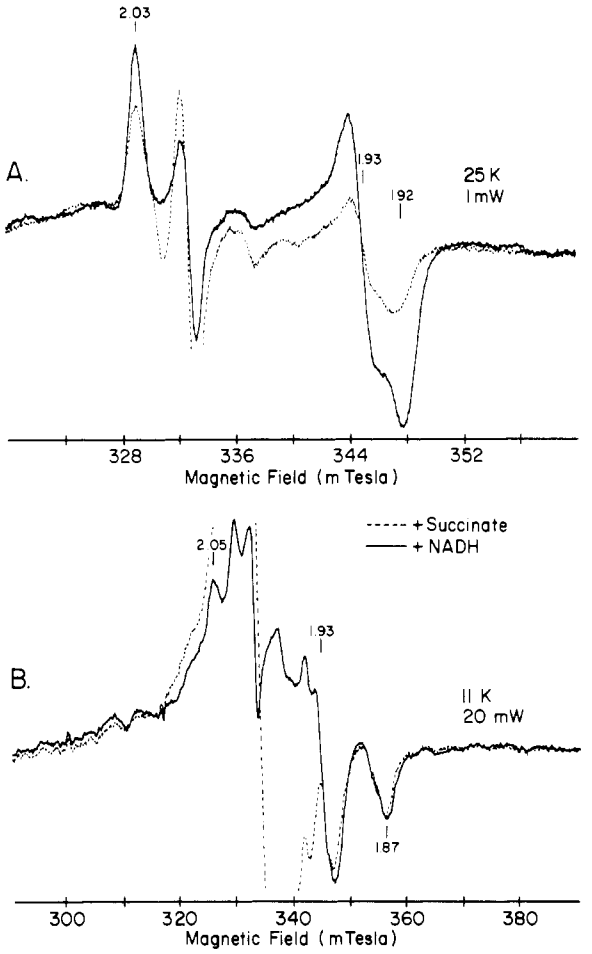

FIGURE 7: Low-temperature EPR spectra of succinate- or NADH-reduced iron–sulfur clusters of *E. coli* IY91. Membrane particles of *E. coli* IY91 were suspended in buffer C and reduced with either NADH, 5 mM final concentration, or succinate, 10 mM final concentration, as indicated. EPR conditions: (A) microwave power, 1 mW; modulation amplitude, 1.25×10^{-3} T; scan rate, 1×10^{-2} T/min; time constant, 0.128 s; temperature, 25 K. EPR conditions: (B) microwave power, 20 mW; modulation amplitude, 8×10^{-4} T; scan rate, 2.5×10^{-2} T/min; time constant, 0.128 s; temperature 11 K.

1.94 signal of the cluster $[N\text{-}3]_E$ has been shifted toward a slightly lower g value ($g = 1.93$) and is also significantly diminished in amplitude relative to the $g_x = 1.87$ signal. Likewise, the E_m of $[N\text{-}3]_E$ was considerably raised as was cluster $[N\text{-}2]_E$. These results indicate that the changes in the NADH dh I gene(s) have resulted in modifications of all fast spin relaxing iron–sulfur clusters, $[N\text{-}2]_E$, $[N\text{-}3a]_E$, and $[N\text{-}3b]_E$.

Discussion

We have demonstrated the presence of at least four different species of low-potential iron–sulfur clusters in *E. coli* GR19N membranes. One cluster, $[N\text{-}1]_E$, is binuclear with a midpoint redox potential of −220 mV and has a rhombic spectrum with $g_{x,y,z}$ values of 1.92, 1.935, 2.03. One tetranuclear cluster, $[N\text{-}2]_E$, has an $E_{m7.4}$ of −240 mV and an almost axial spectrum with $g_{x,y,z} = 1.90, 1.91, 2.05$. The other two iron–sulfur species, $[N\text{-}3a]_E$ and $[N\text{-}3b]_E$ (which have not been assigned as being either binuclear or tetranuclear clusters), have a midpoint potential of −260 mV, pH 7.4, follow $n = 2$ oxidation reduction reaction and have ($g_\perp$, $g_\parallel$) values of (1.94, 2.02) and (1.94, 2.03), respectively. A two-electron oxidation reduction curve for an iron–sulfur cluster is unusual and may indicate that these iron–sulfur clusters are in equilibrium with a redox component that accepts two electrons at a time, such as a flavin

Scheme I: Summary of the Electron-Transport Chain of *E. coli* GR19N[a]

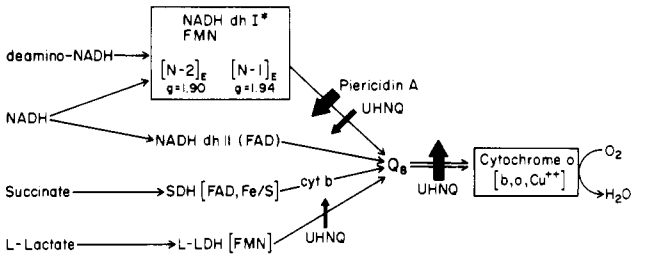

[a] Presented is a brief, tentative scheme of the electron-transport chain of *E. coli*. Enclosed portions show the energy coupling sites in the respiratory chain. The arrows indicate the reactions that are inhibited by either UHNQ or piericidin A. The size of the arrow indicates the relative effectiveness of the inhibitor. The asterisk indicates that two additional low-temperature-detectable $g = 1.94$ iron–sulfur clusters, $[N\text{-}3a]_E$ and $[N\text{-}3b]_E$, might also be part of this complex.

or quinone, or that there is cooperativity between these two clusters in their oxidation reduction reactions.

The results presented here clearly demonstrate that the tetranuclear iron–sulfur cluster $[N\text{-}2]_E$, with $g_{x,y,z} = 1.90, 1.91, 2.05$, is part of the NADH dh I complex. This is supported by its location in the respiratory chain on the substrate side of the piericidin A inhibition site and a close correlation between the loss of the signal and the loss of enzyme activity. In kinetic studies the $g_x = 1.90$ signal is fully reduced by deamino-NADH in less than 17 s, in the presence of piericidin A, and less than 50 s in the absence of any inhibitors (data not shown), which also supports the assignment of this cluster to NADH dh I. The assignment of the binuclear cluster, $[N\text{-}1]_E$, with $g_{x,y,z} = 1.92, 1.935, 2.03$ to this enzyme is supported by the same evidence as given for the $g_x = 1.90$ cluster. The kinetic analysis of its reduction shows, however, that in the presence of piericidin A it is reduced much more slowly than the $g_x = 1.90$ signal, with a half-time of approximately 1 min. The ratio of this cluster to S-1 is quite variable in different batches of the *E. coli* membrane preparations, as is the deamino-NADH activity, and ranges from 1:5 (N-1:S-1) to 1:1. The cluster $[N\text{-}1]_E$ appears to be most vulnerable to the protein modification by the endogenous proteinase of the cells.

The remaining iron–sulfur clusters $[N\text{-}3a]_E$ and $[N\text{-}3b]_E$ may also be part of the NADH dh I complex. Although they are not rapidly reduced in the presence of piericidin A, their redox and spectral properties were modified in the strain IY91, which also lacks deamino-NADH dehydrogenase activity (Matsushita et al., 1987). In the parent strain IY12 from which IY91 was constructed, the loss of all NADH dehydrogenase activity must have been the result of at least two mutations in the genome, and it is quite possible that mutations also occurred at other places. Because of this, it is very difficult to draw any firm conclusions about the location of these iron–sulfur clusters. We have investigated the possibility that these clusters may be part of the formate dehydrogenase complex (Enoch & Lester, 1975) and have found there is little to no formate oxidase activity in *E. coli* GR19N membrane particles when grown with L-lactate as the carbon source. Addition of formate to membrane particles resulted in the reduction of a very small portion of the iron–sulfur cluster in the membrane (less than 10%). Presently the only other complex to which these clusters may be assigned is the D-amino-acid dehydrogenase (Olsiewski et al., 1980). We are now investigating this possibility. Unfortunately, the spectral properties of the iron–sulfur clusters in both the isolated formate dehydrogenase and the D-amino-acid dehydrogenase complexes have not been examined.

The NADH dehydrogenase complex has not been extensively studied in bacterial systems. The *Thermus thermophilus* HB-8 NADH dehydrogenase (Ohnishi et al., 1988a,b) contains at least one binuclear and two tetranuclear iron–sulfur clusters. In contrast to the *E. coli* complex, the *T. thermophilus* complex is extremely thermostable. The *E. coli* and *T. thermophilus* complexes differ from the mitochondrial NADH dehydrogenase (Orme-Johnson et al., 1974; Albracht et al., 1977; Ohnishi, 1979; Hearshen et al., 1981) in that they do not contain an equivalent to the mitochondrial cluster N-2 that has been indicated to play an important role in the coupling of the NADH dehydrogenase to the generation of an electrochemical proton motive force (DeVault, 1976; Ohnishi & Salerno, 1982; Ragan, 1987). On the other hand, *Paracoccus denitrificans* (Albracht et al., 1980; Meinhardt et al., 1987) and *Rhodobacter capsulatus* (Meinhardt and Ohnishi, unpublished results) have NADH dehydrogenase complexes similar to mitochondria, including the presence of a mitochondrial N-2 like cluster. The NADH dehydrogenase complex has been isolated from both *P. denitrificans* (Yagi, 1986) and *T. thermophilus* (Yagi et al., 1988). In each case the complex is much simpler in subunit composition than the mitochondrial complex, having approximately half the number of subunits.

In Scheme I we present our current view of the electron-transport chain in *E. coli* GR19N. The electron transport chain is composed of a series of parallel dehydrogenase complexes of which only a few are presented. The dehydrogenases reduced ubiquinone 8, which is in turn oxidized by cytochrome *o* complex in this strain. The cytochrome *d* ubiquinol oxidase complex (not shown) acts as an alternative oxidase under oxygen limitation in the wild type and has been genetically removed from this strain. NADH dh I is composed of at least two iron–sulfur clusters. It appears that the binuclear cluster $[N\text{-}1]_E$ is near the ubiquinone reaction site since its line shape is modified by the addition of piericidin A, a strongly binding quinone analogue inhibitor. No difference was seen in the line shape of the $g_x = 1.90$ signal of $[N\text{-}2]_E$ when it was resolved kinetically in the presence or absence of inhibitors. The tetranuclear cluster, $[N\text{-}2]_E$, appears to be near the NADH reaction site or its oxidation is the rate-limiting step since it is not modified by the addition of piericidin A. It is also the most rapidly reduced species in the absence or presence of inhibitors (unpublished data). The role of the two remaining fast spin relaxing iron–sulfur clusters, $[N\text{-}3a]_E$ and $[N\text{-}3b]_E$, in the electron-transport chain is at present unclear. Future studies using genetically manipulated strains of *E. coli* should lead to the determination of their role in the electron-transport chain.

Registry No. NADH–ubiquinone reductase, 9028-04-0.

References

Albracht, S. P. J., Dooijewaard, G., Leeuwerik, F. J., & Van Swol, B. (1977) *Biochem. Biophys. Acta 459*, 300–317.

Albracht, S. P. J., Van Verseveld, H. W., Hagen, W. R., & Kalkman, M. L. (1980) *Biochim. Biophys. Acta 593*, 173–186.

Blum, H., & Ohnishi, T. (1980) *Biochim. Biophys. Acta 621*, 9–18.

Bragg, P. D., & Hou, C. (1967) *Arch. Biochem. Biophys. 119*, 202–208.

Brookman, J. J., Downie, J. A., Gibson, F., Cox, G. B., & Rosenberg, H. (1979) *J. Bacteriol. 137*, 705–710.

DeVault, D. (1976) *J. Theor. Biol. 62*, 115–139.

Dutton, P. L. (1978) *Methods Enzymol. 54*, 411-435.
Enoch, H. G., & Lester, R. L. (1975) *J. Biol. Chem. 250*, 6693-6705.
Futai, M., & Kimura, H. (1977) *J. Biol. Chem. 252*, 5820-5827.
Green, G. N., & Gennis, R. B. (1983) *J. Bacteriol. 154*, 1269-1275.
Gutman, M., Schejter, A., & Avi-dor, Y. (1968) *Biochim. Biophys. Acta 162*, 506-517.
Hearshen, D. O., Dunham, W. R., Albracht, S. P. J., Ohnishi, T., & Beinert, H. (1981) *FEBS Lett. 133*, 287-290.
Hendler, R. W., & Burgess, A. H. (1974) *Biochim. Biophys. Acta 357*, 215-230.
Ingledew, W. J., Reid, G. A., Poole, R. K., Blum, H., & Ohnishi, T. (1980) *FEBS Lett. 111*, 223-227.
Jaworowski, A., Campbell, H. D., Poulis, M. I., & Young, I. G. (1981a) *Biochemistry 20*, 2041-2047.
Jaworowski, A., Mayo, G., Shaw, D. C., Campbell, H. D., & Young, I. G. (1981b) *Biochemistry 20*, 3621-3628.
Matsushita, K., & Kaback, H. R. (1986) *Biochemistry 25*, 2321-2327.
Matsushita, K., Ohnishi, T., & Kaback, H. R. (1987) *Biochemistry 26*, 7732-7737.
Meinhardt, S. W., Kula, T., Yagi, T., & Ohnishi, T. (1987) *J. Biol. Chem. 262*, 9147-9153.
Ohnishi, T. (1979) in *Membrane Proteins in Energy Transduction* (Capaldi, R. A., Ed.) pp 1-87 Marcel Dekker, New York.
Ohnishi, T., & Salerno, J. C. (1982) in *Iron-Sulfur Proteins* (Spiro, T. G., Ed.) Vol. 4, pp 285-327, Wiley, New York.
Ohnishi, T., Matsushita, K., Kaback, H. R., Hon-nami, K., & Oshima, T. (1986) in *Iron-sulfur Proteins Research* (Matsubara, H., Ed.) pp 232-239, Japan Scientific Societies Press, Tokyo.
Ohnishi, T., Meinhardt, S. W., Matsushita, K., & Kaback, H. R. (1987) in *Structure and Function of Energy Transducing System* (Ozawa, T., & Papa, S., Eds.) pp 19-29, Japan Scientific Societies Press, Tokyo.
Ohnishi, T., Meinhardt, S. W., Yagi, T., & Oshima, T. (1988a) in *Advances in Membrane Biochemistry and Bioenergetics* (Kim, C. H., Tedeschi, H., Diwan, J. J., & Salerno, J. C., Eds.) pp 237-298, Plenum, New York.
Ohnishi, T., Meinhardt, S. W., Wang, D.-C., Yagi, T., & Hon-nami, K. (1988b) *Proc. 5th EBEC Meet.*, 143.
Olsiewski, P. J., Kaczorowski, G. J., & Walsh, C. (1980) *J. Biol. Chem. 255*, 4487-4494.
Orme-Johnson, N. R., Hansen, R. E., & Beinert, H. (1974) *J. Biol. Chem. 249*, 1922-1927.
Owen, P., & Kaback, H. R. (1979) *Biochemistry 18*, 1413-1422.
Owen, P., Kaczorowski, G. J., & Kaback, H. R. (1980) *Biochemistry 19*, 596-600.
Poole, R. K., & Haddock, B. A. (1975) *Biochem. J. 152*, 537-546.
Ragan, C. I. (1987) *Curr. Top. Bioenerg. 15*, 1-36.
Rainnie, D. J., & Bragg, P. D. (1973) *J. Gen. Microbiol. 77*, 339-349.
Yagi, T. (1986) *Arch. Biochem. Biophys. 250*, 302-311.
Yagi, T., Hon-nami, K., & Ohnishi, T. (1988) *Biochemistry 27*, 2008-2013.
Young, I. G., Jaworowski, A., & Poulis, M. I. (1978) *Gene 4*, 25-36.

In Vivo Enzymology: A Deuterium NMR Study of Formaldehyde Dismutase in *Pseudomonas putida* F61a and *Staphylococcus aureus*†

Ralph P. Mason and Jeremy K. M. Sanders*
University Chemical Laboratory, Lensfield Road, Cambridge CB2 1EW, United Kingdom
Received April 20, 1988; Revised Manuscript Received October 4, 1988

ABSTRACT: High-resolution deuterium NMR spectroscopy has been used to follow the detoxifying metabolism of [D_2]formaldehyde in vivo in several bacterial species. Production of [D_2]methanol in *Escherichia coli* confirms that the oxidation and reduction pathways of metabolism are independent in this organism. Efficient production of equimolar quantities of [D]formate and [D_3]methanol in *Pseudomonas putida* F61a and *Staphylococcus aureus* implicates a formaldehyde dismutase, or "cannizzarase", activity. These observations imply that the unusual formaldehyde resistance in *P. putida* F61a is a direct result of efficient dismutation acting as a route for detoxification. Cross-dismutation experiments yield an enzymic kinetic isotope effect of ca. 4 for H vs D transfer and a similar spectrum of substrate specificity to the isolated enzyme. [D]benzyl alcohol produced by cross-dismutation of [D_2]formaldehyde and benzaldehyde in *P. putida* is demonstrated to have the *R* configuration by a novel deuterium NMR assay. Additionally, *S. aureus* produces methyl formate as a product of formaldehyde detoxification, apparently by oxidizing the methanol hemiacetal of formaldehyde.

Our understanding of the mechanisms of action of enzymes has largely come from studies of isolated material in well-defined, but artificial, media. However, enzymes actually operate in the context of the living cell, so it seems worthwhile to try to study enzyme kinetics and mechanism in this more "natural" environment. NMR[1] spectroscopy is potentially a powerful tool for this type of work, because it is both nonin-

† Financial support from the Science and Engineering Research Council and Unilever Research Ltd. is gratefully acknowledged.

[1] Abbreviations: *B. catarrhlis*, *Branhamella catarrhlis*; *E. coli*, *Escherichia coli*; LADH, horse liver alcohol dehydrogenase; NAD, nicotinamide adenine dinucleotide; NMR, nuclear magnetic resonance; *P. putida*, *Pseudomonas putida*; *S. aureus*, *Staphylococcus aureus*; *S. mutans*, *Streptococcus mutans*; TLC, thin-layer chromatography.

0006-2960/89/0428-2160$01.50/0